Azhar Int J Pharm Med Sci 2025; Vol 5 (2):168-178
Research Article

Open Acces

Print ISSN: 2735-4598
Online ISSN: 2735-4601

Anti-Proliferative Assessment of New Chalcone/Pyridine Linked Urea Fragment: Design, Synthesis and *In Silico* Investigation

Basma A. Abdelkhalek[1*], Mona H. Ibrahim[1], Magda M. F. Ismail[1]

[1] Department of Pharmaceutical Medicinal Chemistry and Drug Design, Faculty of Pharmacy (Girls), Al-Azhar University, Cairo 11754, Egypt.

* Correspondence: bassmazamly2020@gmail.com

Article history: Received: 28-10-2024 **Revised:**13-12-2024 **Accepted:** 10-02-2025

Abstract: As antiproliferative drugs, novel chalcones and pyridine-3-carbonitriles tethered urea were developed. They are effectively synthesised and have the necessary pharmacophoric characteristics to bind to the VEGFR-2 active pocket correctly. The corresponding dihydropyridine-3-carbonitriles **6** and **7** were obtained by condensing the new chalcones **4** and **5** with malononitrile/cyanothioacetamide. The novel compounds were thoroughly characterised using various spectroscopic techniques, including ^{1}H, ^{13}C-NMR, and IR. Additionally, the entire NCI 60 cancer cell panel was used to assess these compounds for their in vitro cytotoxicity properties. Compound **5** (NSC D-852427/1) demonstrated exceptional anticancer activity against the majority of the tested cell lines from the nine distinct subpanels. It shows strong activity against leukaemia in terms of sensitivity to certain cell lines. The evaluated drugs' docking capabilities against VEGFR-2 (PDB ID: 2OH4) were comparable to those of sorafenib. To decipher the target drugs' binding mechanism in the VEGFR-2 pocket, molecular docking studies were used. Furthermore, *in silico* analyses demonstrated that our compounds are not P-gp protein substrates and adhere to the Lipiniski and Veber rules.

Keywords: Design, synthesis; chalcone, pyridine-3-carbonitrile, anti-proliferative; *in silico.*

1. INTRODUCTION

Cancer ranks as one of the major causes of mortality globally. In 2022, about 20 million new cancer cases and 9.7 million cancer-related fatalities occurred globally. According to projections, there will be 35 million new instances of cancer year by 2050 [1]. Timely identification, prophylaxis, and improved therapy are essential to mitigate cancer's effects on individuals and society [2]. In the contemporary medicinal landscape, non-fused pyridines have occurred as a significant classification of heterocycles, characterized by their various pharmacological activity and therapeutic effects. Multiple pyridine-linked ureases have received FDA approval as anticancer agents, including Sorafenib I and Regorafenib II (Figure 1) [3]. Consequently, significant works have been dedicated to developing numerous pyridine-based compounds as potent anticancer medications. Cyanopyridine derivatives have a variety of pharmacological actions, including antibacterial, anticonvulsant, and antiviral activities, as well as enzyme inhibitory properties [4,5]. It is regarded as one of the most distinct foundations of drug discovery. A number of cyanopyridine molecules have been examined for their potential anticancer properties, particularly the compounds III-X (Figure 1). Compound III demonstrated the greatest efficacy against human cell lines of prostate carcinoma PC3 (IC_{50}= 4.82µM), hepatocellular carcinoma HepG2 (IC_{50}= 5.19µM), and breast adenocarcinoma MCF-7 (IC_{50}= 8.17µM), against to the positive control 5-fluorouracil (IC_{50}= 7.53, 8.15, and 7.76 µM, respectively) [6]. Moreover, compounds IVa-c displayed broad-spectrum effectiveness towards nine subpanels of cancer (GI_{50} 0.176-8.87 µM), whereas IVb elicited potent anticancer effect with GI_{50} < 3 µM across many cancer cells, GI_{50} ranging from 0.325 to 2.9 µM [7]. The cyanopyridine derivative V, with a 4-N,N-dimethyl phenyl ring of the pyridine moiety, had notable anticancer activity towards PC-3 (IC_{50} = 0.99 µM), exhibiting eightfold effectiveness compared to staurosporine (IC_{50} = 8.03 µM) [8]. Furthermore, compound VI demonstrated greater potency against HCT-116 (IC_{50} = 7.15 µM) contrasted to 5-FU (IC_{50}

Cite this article: Abdelkhalek B.A., Ibrahim M.H., Ismail M.M.. Anti-Proliferative Assessment of New Chalcone/Pyridine Linked Urea Fragment: Design, Synthesis and *In Silico* Investigation. Azhar International Journal of Pharmaceutical and Medical Sciences, 2025; 5(2):168-178. doi: 10.21608/aijpms.2025.331899.1297

DOI : 10.21608/aijpms.2025.331899.1297

https://aijpms.journals.ekb.eg/

= 8.01 µM) [9]. Additionally, the non-fused carbonitrile compound VII displayed notable antiproliferative effects toward the MCF-7 cells (IC_{50} = 1.39 µM) in comparison to the positive control taxol (IC_{50} = 8.48 µM). Compounds VIII had significant antiproliferative action, with a GI_{50} value of 25 nM versus the tested four cancer cell lines (pancreatic cancer (Panc-1), colon cancer (HT-29), a lung cancer (A-549), and breast cancer (MCF-7)), in comparison to the standard erlotinib, which has a GI_{50} value of 33 nM [10]. Derivative IX demonstrated the highest efficacy against the SKMEL 28, RKOP 27, HeLa, U937, and NCIH 460 cell lines, as indicated by the IC_{50} values of 25, 16, 127, 422, and 255 nM, respectively [11]. Carbonitrile X elicited against the highest inhibitory potency against the proliferation of PC-3 cancer cell lines, with an IC_{50} value of 2.04 µM [12]. Furthermore, chalcone is a fundamental chemical compound that demonstrates anticancer properties, with its effectiveness documented in breast, cervical, and colon malignancies [13]. Figure 2 displays reported anticancer chalcones compounds. Chalcone derivative with OH group compound XI showed IC_{50} = 32.1 µM against a pancreatic cell line [14]. The anticancer screening findings revealed that the synthesized compounds XIIa-d had GI_{50} of < 10 µg/mL toward the breast cancer Cells of human MDA-MB-231[15]. Compound XII revealed powerful anticancer activity its GI_{50} value was 1.33 µM against MCF-7SC cells (Breast Cancer Cell Line) [16]. Moreover, chalcone compound XIII showed antineoplastic activity (GI_{50} = 5.43 µM for MCF7 and GI_{50} = 1.80 µM for HepG2) [17]. Considering the notable anticancer properties of previously discussed pyridine /Chalcone derivatives, our research aimed to design and synthesize targeted anticancer agents as VGFR2 inhibitors.

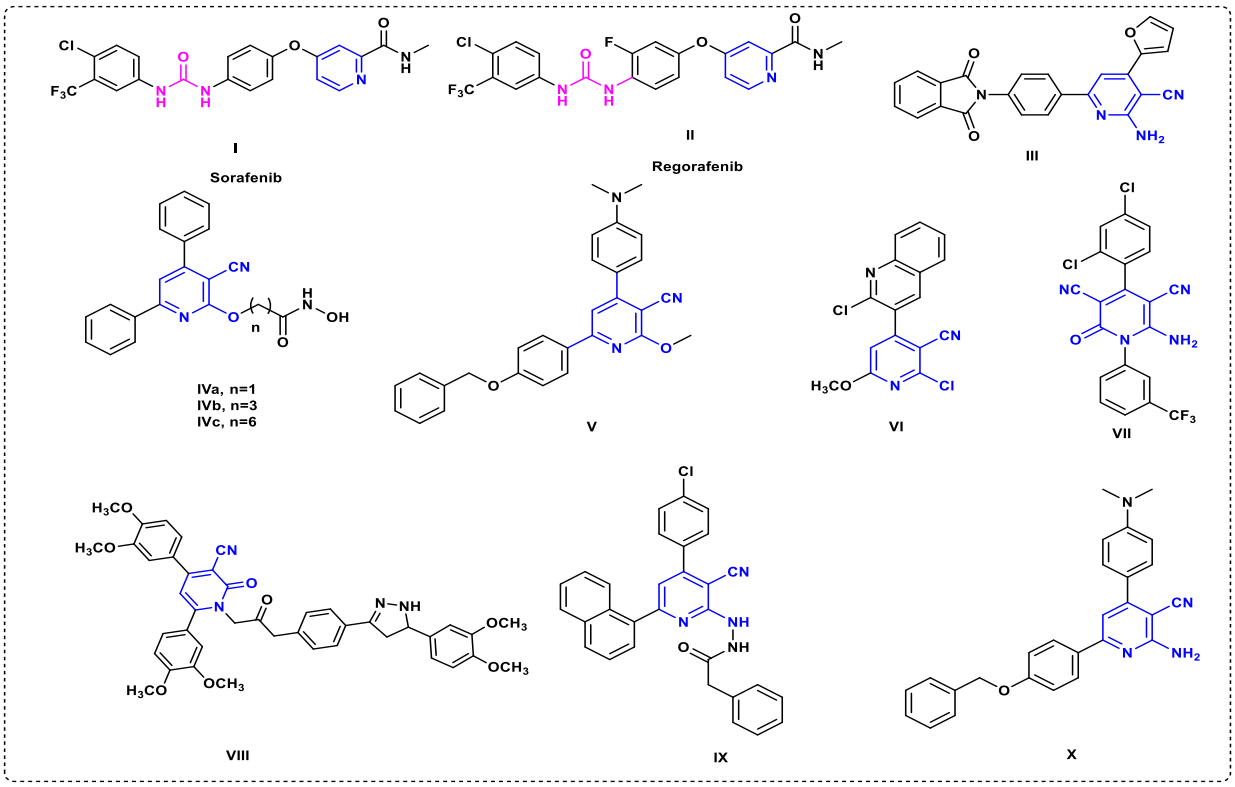

Figure 1. Drugs and reported pyridine-based compounds as anticancer agents.

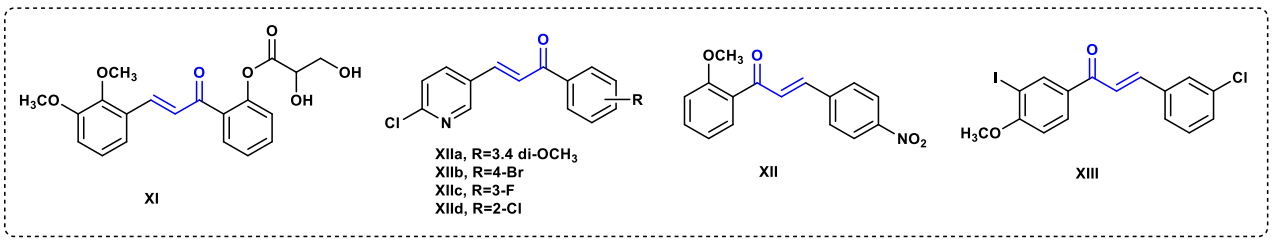

Figure 2. Reported Chalcone-based compounds as anticancer agents.

Rationale

Previous articles have identified four significant pharmacophoric characteristics of VEGFR-2 inhibitors. (i) An heteroaromatic ring with the ability to interact with Cys917 at the hinge point [18]. (ii) A spacer part that can be pointed within the active site's spacer area [19]. (iii) A pharmacophore moiety that can attach to Glu883 and Asp1044 in the DFG motif area, such as an amide or urea (iv) The allosteric site of the VEGFR-2 contains a hydrophobic group [20]. Important scaffolds of remarkable importance in the realm of drug synthesis and discovery are pyridines and chalcones. These scaffolds have been seen in a number of documented anticancer medications, including VEGFR-2 inhibitors. The pyridine moiety is involved in two FDA-approved VEGFR-2 inhibitors, Regorafenib I and Regorafenib II, which form a hetero-aromatic system. A number of VEGFR-2 drugs were designed using ligand-based drug design. As shown in **Figure 3**, the spacer group was kept as a phenyl ring, just like in sorafenib, and the heteroaromatic system was intended to be either chalcone or a cyclized form of it (pyridine). All of the proposed compounds retained the urea group as the pharmacophore moiety and the phenyl ring as the terminal hydrophobic moiety.

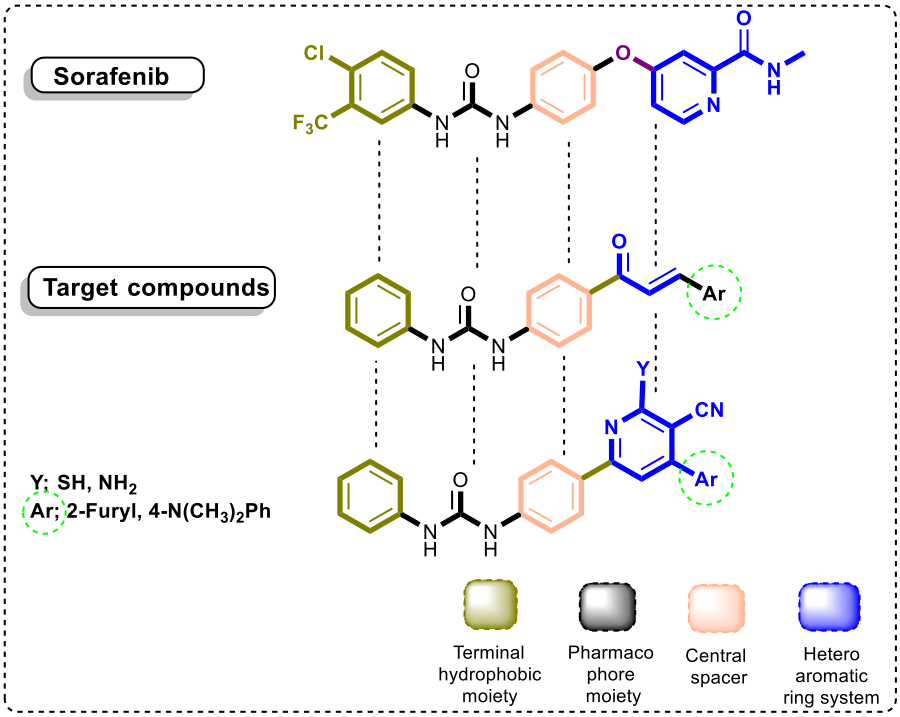

Figure 3. Rationale of our compounds as VEGFR2 inhibitors

2. METHODS

2.1. Chemistry

All information about apparatuses was mentioned in the supplementary file.

Synthesis of 1-(4-acetylphenyl)-3-phenylurea (3)

Dry toluene (20 ml) was used to dissolve a mixture of phenylisocyanate 1 (10 mmol) and 4-aminoacetophenone 2 (10 mmol). Dry toluene was introduced to the mixture after it was refluxed overnight **(Scheme 1).** The resultant powder was dissolved, and recrystallization yielded the required 1-(4-acetylphenyl)-3-phenylurea **3** in pure form, exhibiting a melting temperature of 172-175 °C as documented [21].

Synthesis of compounds:

1-(4-(3-(4-(Dimethylamino)phenyl)acryloyl)phenyl)-3-phenylurea (4) and 1-(4-(3-(furan-2-yl)acryloyl)phenyl)-3-phenylurea (5)

The synthesis of phenylurea-substituted chalcone derivatives was achieved by reacting equimolar amounts of compound **3** with the respective Furan-2-carboxaldehyde or 4-N, N-dimethylaminobenzaldehyde. An extra of NaOH (2.5 mmol) was used in dry methanol (10 ml) and dimethylsulphoxide (10 ml). A 30 ml frigid brine was added to the mixture after the solution was stirred at room temperature overnight. The precipitate that

forms was subsequently filtered and air-dried [22]. Pure phenylurea-substituted chalcones were obtained by recrystallizing the precipitate from the appropriate solvent. **4-5 (Scheme 1, Table 1)**.

1-(4-(6-Amino-5-cyano-4-(4-(dimethylamino)phenyl)-4,5-dihydropyridin-2-yl)phenyl)-3-phenylurea (6)

The synthesis of 6-amino-5-cyano-4,5-dihydropyridine was accomplished by recirculating 0.05 M of the appropriate chalcone, 0.05 M of malononitrile, and 0.36 M of ammonium acetate in 100% ethanol (90 mL) over a period of time ranging from 5-7 h. Filtration, washing with ethanol, drying, and recrystallization from ethanol were the steps that were taken to get the precipitate [12], as shown in **Scheme 2**.

1-(4-(5-Cyano-4-(4-(dimethylamino)phenyl)-6-thioxo-1,4,5,6-tetrahydropyridin-2-yl)phenyl)-3-phenylurea (7)

The target compound 6-thio-5-cyano-4,5-dihydropyridine, was synthesized by refluxing the respective chalcone (0.05 mole), cyanothioacetamide (0.15 g, 0.05 mole), and piperidine in 100% ethanol (80 mL) for 5 to 7 h. The resultant precipitate was then rinsed with ethanol, dried, and recrystallized from ethanol [8], as seen in **(Scheme 2, Table 1).**

Table 1: Yield, m.p, IR**(cm^{-1}), ^{1}H-NMR and ^{13}C-NMR** (DMSO-d_6) δ (ppm), MS m/z % of the target compounds

Cpd	Yield%	m.p.°C	IR (KBr) (cm^{-1})	^{1}H-NMR (DMSO-d_6) δ (ppm)	^{13}C-NMR (DMSO-d_6) δ (ppm)	MS m/z (%)
4	85	180-182	3342 (NH), 3304 (NH), 1658(CO), 1637 (CO);	3.01 (s, 3H, NCH_3), 3.05 (s, 3H, NCH_3), 6.73 (d, 2H, aryl-H, *J*=8 Hz), 6.94 (t, 1H, phenylurea-H, *J*=8 Hz), 7.21 (t, 2H, phenylurea-H), 7.50 (d, 2H, aryl-H, *J*=8 Hz), 7.57-7.67 (m, 5H, 2H, AB system-H, 1H, enone-H, 2H, phenylurea-H), 7.81 (d, 2H, AB system-H, *J*=8 Hz), 7.96 (d, 1H, enone-H, J=8 Hz), 9.75 (br s, 2H, 2NH, D2O exchangeable)	56.48 (2$\underline{C}H_3$), 113.60 (2C), 117.21 (1C), 117.87 (1C), 118.69 (1C), 118.94 (1C), 119.07 (2C), 122.44 (enone-C), 122.82 (1C), 129.32 (2C), 130.29 (1C), 130.33 (2C), 131.23 (1C), 139.59 (1C), 144.97 (enone-C), 146.43 (1C), 151.60 (1C), 152.68 (N–$\underline{C}$=O), 187.50 ($\underline{C}$=O)	385.50 (M^+, 46.44), 175.14 (100.00)
5	70	120 - 122	3315, 3122 (2NH), 1653, 1595 (2CO)	6.66 (t, 1H, furan-H, *J*=8 Hz), 7.00 (t, 1H, phenylurea-H, *J*=8 Hz), 7.06 (d, 1H, furan-H, *J*=8 Hz), 7.29 (t, 2H, phenylurea-H, *J*=8 Hz), 7.43 (d, 2H, AB system-H, *J*=8 Hz), 7.54 (d, 1H, enone-H, *J*=8 Hz), 7.63 (d, 2H, AB system-H, *J*=8 Hz), 7.86 (d, 1H, enone-H, *J*=8 Hz), 8.03 (d, 1H, furan-H, *J*=8 Hz), 9.50 (br s, 2H, 2NH, D2O exchangeable)	111.48 (1C), 112.23 (1C), 116.15 (1C), 117.71 (1C), 119.05 (1C), 122.33 (1C), 122.41 (1C), 122.60 (enone-C), 129.19 (1C), 130.03 (1C), 130.42 (enone-C), 131.10 (1C), 131.71 (1C), 139.91 (1C), 139.93 (1C), 144.95 (1C), 145.02 (1C), 145.36 (1C), 153.20 (C=O) 190.92 (N–C=O)	332.35 (M^+, 9.09), 122.79 (100.00)
6	75	188-190	3299, 3209, 3105 (NH_2, 2NH), 2216 (CN), 1642 (CO)	2.6 (d, 1H, H3, pyridine-H), 3.01 (s, 3H, $NC\underline{H}_3$), 3.09 (s, 3H, $NC\underline{H}_3$), 3.8 (m, 1H, H4, pyridine-H), 6.85 (d, 2H, Ar-H, J=8 Hz), 6.99-7.03 (m, 2H, 1H, C_6H_5-H, 1H, H5-pyridine), 7.31 (t, 2H, C_6H_4-H, *J*=8 Hz), 7.48 (d, 2H, Ar-H, *J*=8 Hz), 7.63 (d, 2H, AB system-Ar-H, *J*=8 Hz), 7.71 (d, 2H, AB system-Ar-H, *J*=8 Hz), 7.83 (d, 2H, phenyl-H), 8.25 (s, 1H, NH_2, D_2O exchangeable), 8.86, 9.18 (s, 2H, 2NH, D2O exchangeable)	25.3 (C4-pyridine), 32.9 (C5-pyridine), 44.20 (2C,($N\underline{C}H_3)_2$), 112.25 (1C), 114.58 (1C), 115.15 (1C), 116.41 ($\underline{C}$N), 118.25 (C), 119.05 (2C), 122.31 (1C), 122.31 (1C), 129.58 (2C), 130.22 (1C), 130.14 (C), 131.21 (1C), 131.14 (1C), 139.32 (C), 139.85 (1C), 144.74 (1C), 145.16 (1C), 145.19 (1C), 158.18 (C=O), 158.85 ($\underline{C}$-NH2), 161.53 (1C)	450.55 (M^+, 12.09), 125.58 (100.00)

7	80	199-200	3315 (br s, 3NH), 2186 (CN), 1690 (CO)	2.84 (d, CH-CN), 3.02 (s, 6H, 2NCH$_3$), 3.44 (m, 1H, pyridine-H), 6.75 (d, 2H, H$_{2,6}$, AB system-Ar-H, J=8 Hz), 7.00 (t, 1H, H4, pyridine-H), 7.30 (t, 2H, H3,5, pyridine-H), 7.49 (d, 2H, H$_{2,6}$, C$_6$H$_5$-H, J=8 Hz), 7.60-7.72 (m, 3H, 2H, H$_{3.5}$, aryl-H, H5, pyridine-H), 7.90 (d, 2H, AB system-H-C$_6$H$_4$, *J*=8 Hz), 8.09 (d, 2H, AB system-H-C6H4, *J*=8 Hz), 8.85 (s, 1H, NH, D2O exchangeable), 9.06 (s, 1H, NH, D2O exchangeable), 9.37 (s, 1H, NH-pyridine, D2O exchangeable)	22.60 (C4-pyridine), 26.31 (C3-pyridine), 44.80 (2C-(NCH3)2), 111.28 (1C), 111.84 (1C), 116.61 (1C), 116.91 (CN), 117.06 (1C), 117.20 (1C), 118.16 (1C), 118.38 (1C), 121.28 (2C), 122.30 (1C), 128.52 (2C), 129.27 (1C), 129.48 (1C), 129.53 (1C), 129.83 (1C), 130.75 (1C), 153.43 (C=O), 157.01 (1C), 158.68 (1C), 162.45 (1C), 174.44 (C=S)	467.50 (M^+, 9.70), 215.21 (100.00)

2.2. NCI anticancer screening *in vitro*

The first anticancer experiment was conducted on a panel of roughly sixty human malignant tumour cell lines originating from nine neoplastic disorders, following the procedure established by the Drug Evaluation Branch of the National Cancer Institute in Bethesda. The compounds were evaluated using the updated NCI-60 HTS384 platform.

2.3. *In silico* studies

2.3.1. Prediction of physicochemical and ADME parameters

via the website https://www.rcsb.org/chemical-sketch , the molecular structures were converted into a SMILES database. The physicochemical identifiers, lipophilicity, pharmacokinetic characteristics, ADME variables, and medicinal chemistry compatibility were subsequently calculated by inputting these SMILES into the SwissADME website.

2.3.2. Molecular docking study

A 2.03 Å resolution 3D structure of VEGFR2 was obtained from the Protein Data Bank [PDB ID: 4ASD]. Autodock Vina 4.2 was employed to execute the docking processes. The Discovery Studio 4.5 visualizer was employed to display the results.

3. RESULTS and DISCUSSION

3.1. Chemistry

Schemes 1 and **2** described the process of synthesizing the targeted members. 4-aminoacetophenone, **2** has been added nucleophilically to phenylisocyanate, 1 to synthesize urea derivative, **3**. Chalcones are distinguished by their easy synthesis from Claisen-Schmidt condensation. Chalcones **4**, and **5** were then produced via a condensation reaction between the acetyl functionality of the intermediate, **3**, and the carbonyl group of either furan-2-carbaldehyde or 4-(dimethylamino) benzaldehyde in a basic medium [23]. Clarification of the chalcone's structure Using chalcone **5** as an example, the IR (KBr) spectrum of sample **5** shows two carbonyl bands at 1653 and 1595 cm^{-1}. ^{1}HNMR (DMSO-d_6) δ (ppm) demonstrated the existence of furan moiety, with two doublets at δ 7.06 and 8.3 ppm for H3 and H5, respectively, and a shielding triplet at δ 6.66 ppm. Using ^{13}C NMR (DMSO-d_6), two signals were detected at 153.20 (C=O) and 190.92 (NH-C=O), along with two signals that correspond to two enone-C at δ 122.60 and 130.42 ppm.

Additionally, 6-thioxo-1,4,5,6-tetrahydropyridine-5-carbonitrile **7** was extracted by a one-pot reaction of chalcone **4** and cyanothio-acetamide in ammonium acetate, which provids cyclocondensation of chalcone to pyridine [8,12]. **Scheme 2**'s technique yielded the equivalent 6-amino-4,5-dihydropyridine-5-carbonitrile **6** when malononitrile was used in place of cyanothio-acetamide. As an example of pyridine derivatives, the IR (KBr) spectrum of molecule **6** revealed the absence of the parent chalcone **4**'s carbonyl band and the presence of strong bands at 3299, 3209, and 3105 cm^{-1}, which correspond to NH_2, 2NH, and another strong band at 2216 cm-1, which represents the CN functionality. In addition, ^{1}HNMR (DMSO-d_6) demonstrated the presence of two singlets for N $(CH_3)_2$ protons at δ 3.01 and 3.09 ppm and pyridine-H3 at 2.6 ppm as a multiplet. At δ 3.8 and 6.99-7.03, there were two additional multiplets that correspond to pyridine-H4 and pyridine-H5, respectively. C4-pyridine was also detected at δ 25.3 and C5-pyridine at δ 32.9 in the ^{13}C NMR (DMSO-d_6) spectrum. Moreover, $NCH_3)_2$ was detected at δ 44.20, while the cyano group was detected at δ 116.41ppm.

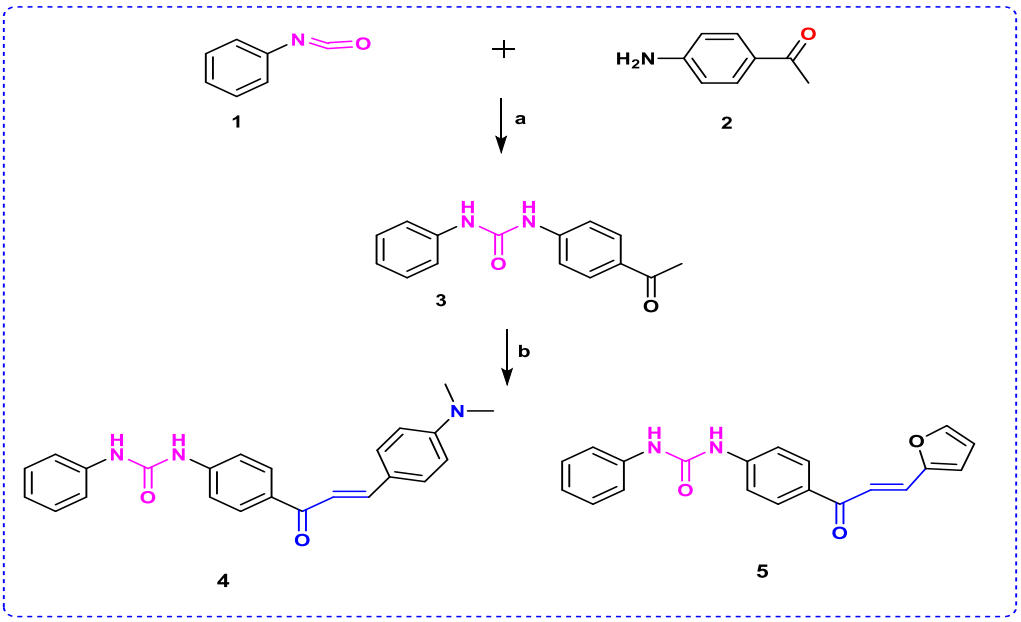

Scheme 1. Reagents and conditions: (a) reflux overnight, (b) Aldehyde derivatives, NaOH sol 60 %, 0°C.

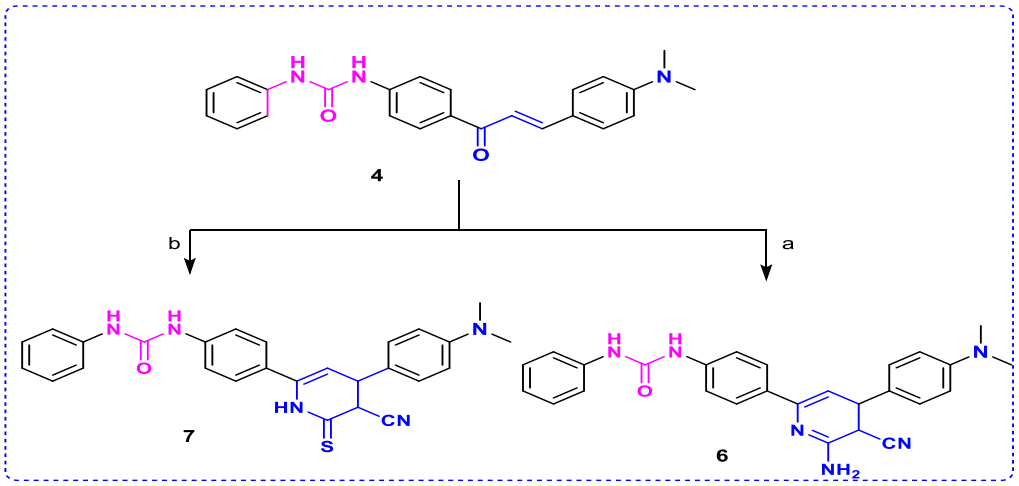

Scheme 2. Reagents and conditions: (a) malononitrile, ammonium acetate, reflux 5-7 h; (b) Cyanothioacetamide, pipredine, reflux 5-7 h.

3.2. *In vitro* anticancer screening

3.2.1. *In vitro* single dose 60-cell line test

The National Cancer Institute (NCI) identified target compounds **4**, **5**, **6**, and **7** for screening against 60 cell line panels to assess their anticancer efficacy. Following the NCI, USA procedure, a primary in vitro single-dose anticancer assay was conducted on the whole NCI 60-cell panel, which include leukemia, melanoma, and tumors of the lung, ovary, brain, prostate, kidney, colon, and breast. A mean graph demonstrating the percentage growth of treated cells compared to untreated control cells was utilized to present the results for each treatment.

Table S1 summarizes the screening outcomes of a single dose-anticancer test. Reviewing the NCI data for our target compounds **4–7** showed that chalcone **5** with the electron-withdrawing group 2-furyl moiety had a strong growth inhibitory effect, whereas chalcone **4** with the electron-releasing group N $(CH_3)_2$Ph had a lesser anticancer effect **(Table S1).**

Among the studied compounds, compound **5** demonstrated the strongest anticancer efficacy; it displayed strong growth inhibitory effect against the

majority of the cell lines (**Figure 4**). It's interesting to note that it reported lethality towards cell subpanels for the majority of leukemia (-96.69 to -78.90), some NSCLC (-86.07 to -38.93), melanoma (-21.54), colon (-25.74 to -16.59), ovarian (-79.45), renal (-56.54), and breast cancer (-18.45). Chalcone **4** was also produced via the bioisosteric substitution of furan with a phenyl ring replaced with an E-releasing moiety (N $(CH_3)_3$). With GI% 92.63-72.3, it showed extremely strong anticancer effectiveness against certain leukemia subpanels. Additionally, it was fatal to SR and RPMI-8226, which showes -94.09 and -24.32, respectively. With the exception of MDA-MB-231/ATCC, all breast panels displaying GI% 95.46–70.95 showed its potency. Similarly, compound **4** had a high GI% inhibition versus NSCLC subpanels; however, it was inactive against NCI-H322M and NCI-H522. Also, there was a good to moderate impact on malignancies of the prostate, ovaries, central nervous system, and kidneys.

All things considered, the anticancer activity against the majority of the cancer panels was not improved by cyclizing chalcone **4** with either malononitrile or cyanothioacetamide to yield the corresponding pyridine derivatives, **6** and **7**, respectively. Among their cytotoxic results, pyridine **6** showed medium range cytotoxicity towards NSCLC-EKVX (GI% 34.72) and leukemia-CCRF-CEM (GI% 37.44), as well as high potency (GI% 70.33) against NSCLC-NCI-H522. In conclusion, the cytotoxicity of 2-thioxopyridine, **7**, its equivalent, was found to be in a moderate range when tested against NSCLC-NCI-H522 (GI% 32.42) and breast-HS578T (GI% 37.31). In terms of cytotoxicity against NSCLC-NCI-H522, it was shown that o-aminonitrile **6** had a greater polarity than its less polar counterpart **7**, with **6** eliciting activity that was more than twice as high as **7, (Supp S1)**.

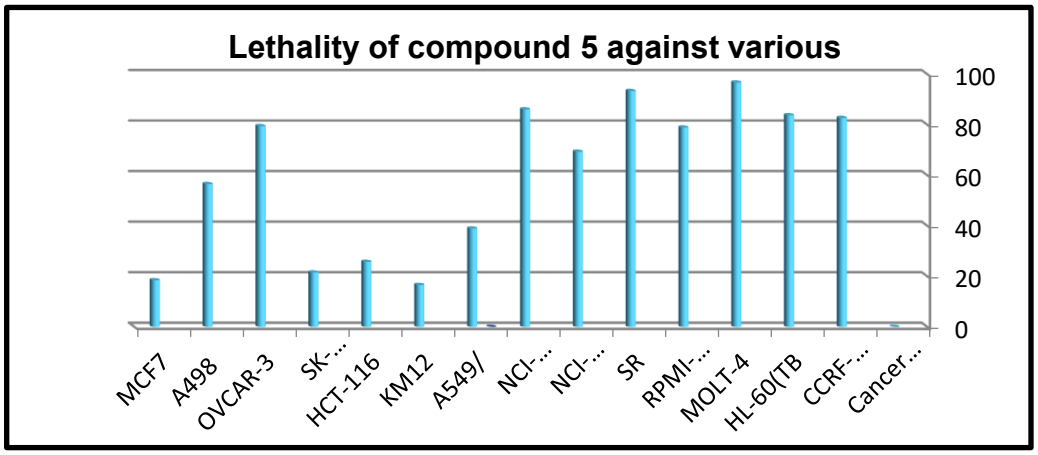

Figure 4. Lethality of compound 5 against various cancer cell lines

3.3. *In silico* studies

3.3.1 Assessment of physicochemical and ADME characteristics

A computational investigation evaluated the physicochemical and ADME characteristics of the synthesized compounds. Utilizing software named SwissADME, it was feasible to ascertain the likelihood of the compounds being bioactive based on several critical parameters, including the Veber and Lipinski rules. The physicochemical features of test compounds, as indicated in **Table 2**, conform to the Lipinski and Veber criteria, displaying no violations. This indicates that these compounds possess favorable drug-like characteristics.

Table 2: physicochemical properties based on Lipinski´s rule of five and the number of rotatable bonds.

Cpd.No.	HBD	HBA	M logP	M.Wt	No. of Rot. bonds	Lipinski´s Violations	Veber's Violations
4	2	2	3.74	385.46	8	0	0
5	2	3	2.25	332.35	7	0	0
6	3	3	2.88	450.53	7	0	0
7	3	2	2.94	467.59	7	0	0
Sorafenib	3	7	2.91	464.82	9	0	0
Linifanib	4	3	4.02	375.40	5	0	0

All compounds adhere to Veber's rule as their computed topological polar surface area (TPSA) values fall within the range that permits transmembrane passage. All compounds exhibit elevated absorption percentages (68.97–87.80%), suggesting the feasibility of oral administration. Sorafenib (77.13) had a lower absorption percentage than compounds **4** (87.8%) and **5** (84.39%) (**Table 3**).

Table 3: the topological polar surface area (TPSA), and % ABS

Cpd. No.	TPSA	% ABS
4	61.44	87.80
5	71.34	84.39
6	106.54	72.06
7	112.28	68.97
Sorafenib	92.35	77.13

The medicinal chemistry characteristics and physicochemical properties of the test molecules were anticipated utilizing SwissADME software. All compounds exhibit good gastrointestinal absorption, except for compound **7**, which demonstrates limited gastrointestinal absorption akin to sorafenib and possesses high bioavailability scores (0.55). Furthermore, compounds **6** and **7**, anticipated to demonstrate BBB penetration, are not expected to trigger any alerts according to SwissADME. Still, compounds **4** and **5**, also predicted to exhibit BBB permeation, should elicit one alert. Additionally, studies conducted by SwissADME indicated that all analogues have synthetic accessibility scores ranging from 3.02 to 3.43, suggesting that their large-scale synthesis is quite uncomplicated. Moreover, they do not serve as substrates for P-glycoprotein. Upon evaluation, it was determined that our compounds possess physicochemical properties and medicinal chemistry criteria that exist suitable, suggesting their potential as medications, as shown in **Table 4.**

Table 4: Pharmacokinetic properties and medicinal chemistry parameters:

Cpd. No.	GI Absorption	BBB Permeation	P-gp substrate	Bioavailability Score	PAINS Alerts	Synthetic Accessibility
4	high	Yes	No	0.55	1	3.14
5	high	Yes	No	0.55	0	3.02
6	high	No	Yes	0.55	1	4.97
7	high	No	Yes	0.55	2	4.59
Sorafenib	low	No	No	0.55	0	2.87

3.3.2 Molecular docking

Docking investigations of compounds **4-7** effectively investigate the potential interactions and affinity relative to the standard molecule, sorafenib, with the VEGFR-2 kinase domain. The docking process was verified by an RMSD of 0.135 Å between the docked compound and the co-crystallized compound, sorafenib, upon redocking in the active site of the VEGFR-2 kinase domain (PDB ID: 4asd). Sorafenib obtained a docking value of -10.25 kcal/mol. Therefore, the enzymatic activity of the compounds that were examined, as well as the construction of substantial contacts with the binding sites and the favorable energy scores that corresponds to those interactions, were dependent on the achievement of a binding conformation that was comparable to that of sorafenib. As a result, the aforementioned scores provided as comparable benchmark values for the docked molecules **4–7**. Sorafenib's gate area contained eight hydrogen bonding interactions, including two donors between the urea nitrogen atom and the Glu885 amino acid, as well as two acceptors between the urea carbonyl oxygen and Asp1046 and Cys1045 (**Fig. S1**). The crucial amino acid Cys919 and two hydrogen bonds with the nitrogen atom were formed by the hinge region, which also interact with Glu917 to promote attachment. Sorafenib demonstrated 14 hydrophobic interactions with Phe1047, Leu889, Val848, Ala866, Lys868, Val899, Val916, Cys1045, Leu840, Val848, Cys919, and Leu1035. The significant inhibitory effects of compounds **4-7** (**Fig. 5-8**, **Supp. Table S2**) are elucidated by their docking scores, which varies between -13.45 and -15.60 kcal/mol. Furthermore, the compounds successfully established the necessary interaction pattern to inhibit VEGFR-2. The urea linker of compounds **5** and **7** elicited one hydrogen bond donor and one hydrogen bond acceptor with Cys919, an essential residue. Compound **4**, with a docking score of -13.73 Kcal/mol, established four hydrogen bonds with Ile1025, His1026, and Cys919, and demonstrated 12 hydrophobic contacts (**Fig. 5**, **Supp. Table S2**). As shown in **Figure 6**, **Supplementary Table S2,** Compound **5** had five hydrogen bonds with Cys919, Lys868, and Phe948 and eight Pi-Alkyl interactions with Leu840, Val848, Ala866, Val899, Val916, Leu1035, and Cys1045. Compounds **6** and **7** displayed Pi-Alkyl interactions with Val848, Ala866, Cys1045, Val899, and Leu1035 (**Fig. 7, 8, Supp Table S2**). The docking scores for compounds **6** and

7 were -15.91 and -15.60 Kcal/mol, respectively. Furthermore, compound **6**, which possesses the highest docking score of -15.91 Kcal/mol, established two hydrogen connections with Val914 and His1026.

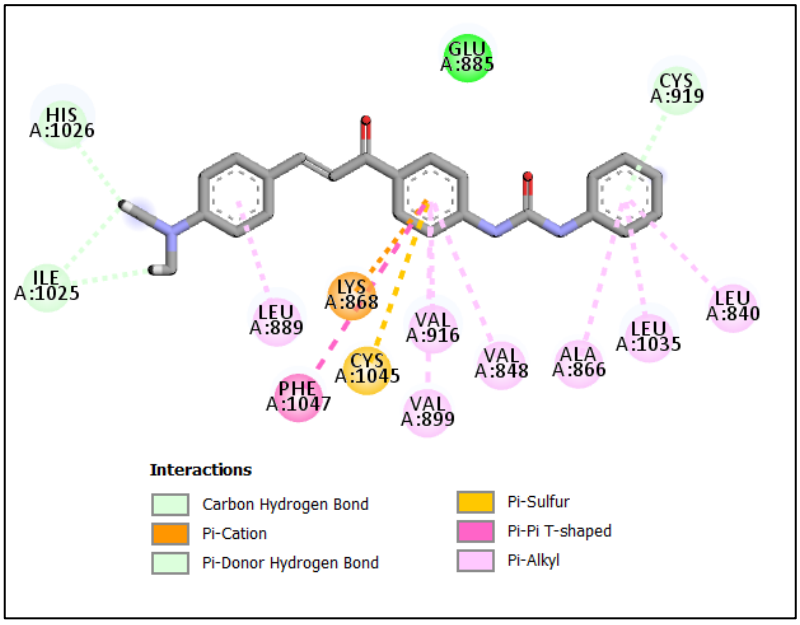

Figure 5. 2D of compound **4** docked into the binding site of VEGFR-2 active site enzyme.

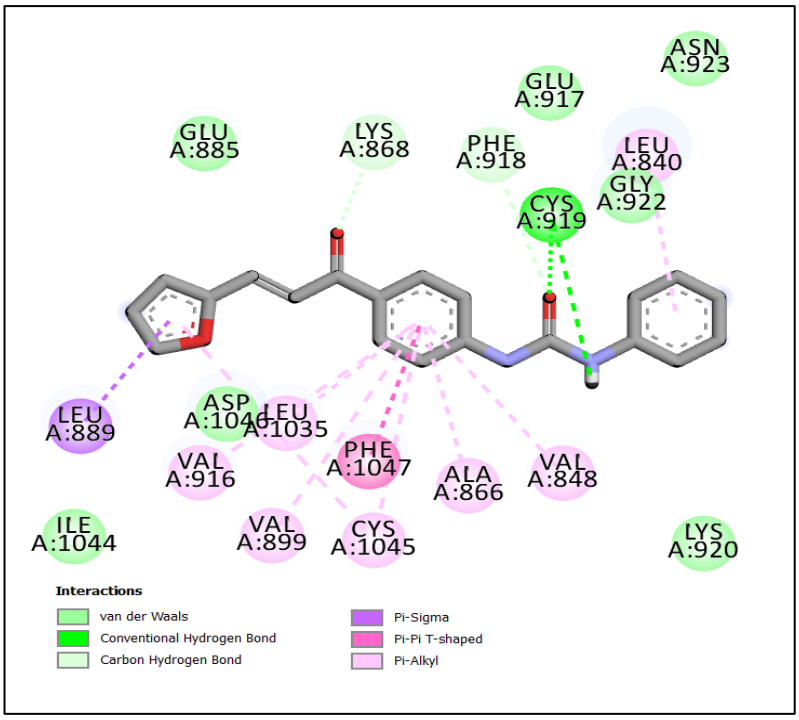

Figure 6. 2D of compound **5** docked into the binding site of VEGFR-2 active site enzyme

4. CONCLUSIONS

Four novel compounds that mimics the observed pharmacophore characteristics of VEGFR-2 inhibitors were developed and synthesized. Based on biological results, compounds **4** and **5** have been identified as particularly interesting cytotoxic agents. Compound **5** stood up as having the most potent cytotoxic activity against the majority of cancer cell lines. Additionally, compounds **6** and **7** showed

modest efficacy against the three cancer subpanels, namely breast cancer, NSCLC, and leukemia. They showed binding patterns similar to those found in the docking experiments for the majority of VEGFR-2 inhibitors. According to the outcomes of the *in silico* prediction, compounds **6** and **7** in particular have a specific degree of freedom in *BBB* penetration. It's interesting to note that none of the compounds are substrates of the P-gp protein, suggesting that their efficacy won't be diminished. In our upcoming work, the novel compounds can be viewed as a good beginning point for further modification and development.

Supplementary Materials: chemistry

Funding: No funding.

Conflicts of Interest: The authors declare no conflict of interest.

Acknowledgement: Cytotoxicity was performed by NCI.

Author Contribution: All authors had full access to all the information and took responsibility for data integrity and data analysis accuracy. Author Magda M. F. Ismail designed the study. Author Basma Abdel Hameed Abdelkhalek performed the experimental work. Authors Mona H. Ibrahim and Basma Abdel Hameed Abdelkhalek wrote the manuscript. NCI performed the cytotoxic activity. Author Magda M. F. Ismail supervised the work and revised the whole manuscript. The final manuscript was read and accepted by all the contributors.

List of Abbreviations: VEGFR-2: Vascular endothelial growth factor receptor-2.; NCI : National Cancer Institute.

REFERENCES

1. Bray F, Laversanne M, Sung H, Ferlay J, Siegel RL, Soerjomataram I, et al. Global cancer statistics 2022: GLOBOCAN estimates of incidence and mortality worldwide for 36 cancers in 185 countries. CA Cancer J Clin. 2024;74:229–263.

2. Barrios CH. Global challenges in breast cancer detection and treatment. Breast. 2022;62:S3-S6.

3. El-Naggar M, Almahli H, Ibrahim HS, Eldehna WM, Abdel-Aziz HA. Pyridine-ureas as potential anticancer agents: Synthesis and in vitro biological evaluation. Molecules. 2018;23:1459-1475.

4. Wu Y, Wu T, Huang Y. A review: Biological activities of novel cyanopyridine derivatives. Archiv der Pharmazie. 2023;356:1-15.

5. Ibrahim MH, El Menofy NG, El kiki SM, Sherbiny FF, Ismail MMF. Development of fluorinated nicotinonitriles and fused candidates as antimicrobial, antibiofilm, and enzyme inhibitors. Archiv der Pharmazie. 2022;355:1-15.

6. Farrag AM, Ibrahim MH, Mehany ABM, Ismail MMF. New cyanopyridine-based scaffold as PIM-1 inhibitors and apoptotic inducers: Synthesis and SARs study. Bioorg Chem. 2020;105:104378-104391.

7. Bass AKA, Nageeb ESM, El-Zoghbi MS, Mohamed MFA, Badr M, Abuo-Rahma GEDA. Utilization of cyanopyridine in design and synthesis of first-in-class anticancer dual acting PIM-1 kinase/HDAC inhibitors. Bioorg Chem. 2022;119:105564-105588.

8. Ibrahim MH, Harras MF, Mostafa SK, Mohyeldin SM, Al kamaly O, Altwaijry N, et al. Development of novel cyanopyridines as PIM-1 kinase inhibitors with potent anti-prostate cancer activity: Synthesis, biological evaluation, nanoparticles formulation and molecular dynamics simulation. Bioorg Chem. 2022;129:106122:106134.

9. Mansour B, Salem YA, Attallah KM, El-Kawy OA, Ibrahim IT, Abdel-Aziz NI. Cyanopyridinone- and Cyanopyridine-Based Cancer Cell Pim-1 Inhibitors: Design, Synthesis, Radiolabeling, Biodistribution, and Molecular Modeling Simulation. ACS Omega. 2023;8:19351-19366.

10. Al-Wahaibi LH, Abou-Zied HA, Hisham M, Beshr EAM, Youssif BGM, Bräse S, et al. Design, Synthesis, and Biological Evaluation of Novel 3-Cyanopyridone/Pyrazoline Hybrids as Potential Apoptotic Antiproliferative Agents Targeting EGFR/BRAFV600E Inhibitory Pathways. Molecules. 2023;28:6586-6606.

11. El-Sayed AA, Elsayed EA, Amr AEGE. Antiproliferative Activity of Some Newly Synthesized Substituted Pyridine

Candidates Using 4-(Aaryl)-6-(naphthalen-1-yl)-2-oxo-1,2-dihydropyridine-3-carbonitrile as Synthon. ACS Omega. 2021;6:7147-7156.

12. Ismail MMF, Farrag AM, Harras MF, Ibrahim MH, Mehany ABM. Apoptosis: A target for anticancer therapy with novel cyanopyridines. Bioorg Chem [Internet]. 2020;94:103481-10394

13. Ouyang Y, Li J, Chen X, Fu X, Sun S, Wu Q. Chalcone derivatives: Role in anticancer therapy. Biomolecules. 2021;11:894-930.

14. Baek S, Nah S, Park JY, Lee SJ, Kang YG, Kwon SH, et al. A novel chalcone derivative exerts anticancer effects by promoting apoptotic cell death of human pancreatic cancer cells. Bioorg Med Chem. 2023;93:117458-117466.

15. Sankhe SS, Mukadam VM. Pyridine-based chalcones as promising anticancer agents: Design, synthesis and in silico studies. Results Chem. 2024;9:101633-101642.

16. Ahn S, Truong VNP, Kim B, Yoo M, Lim Y, Cho SK, et al. Design, synthesis, and biological evaluation of chalcones for anticancer properties targeting glycogen synthase kinase 3 beta. Appl Biol Chem. 2022;65:1-14.

17. Abosalim HM, Nael MA, El-Moselhy TF. Design, Synthesis and Molecular Docking of Chalcone Derivatives as Potential Anticancer Agents. ChemistrySelect. 2021;6:888–895.

18. Lee K, Jeong KW, Lee Y, Song JY, Kim MS, Lee GS, et al. Pharmacophore modeling and virtual screening studies for new VEGFR-2 kinase inhibitors. Eur J Med Chem. 2010;45:5420-5427.

19. Machado VA, Peixoto D, Costa R, Froufe HJC, Calhelha RC, Abreu RMV, et al. Synthesis, antiangiogenesis evaluation and molecular docking studies of 1-aryl-3-[(thieno[3,2-b]pyridin-7-ylthio)phenyl]ureas: Discovery of a new substitution pattern for type II VEGFR-2 Tyr kinase inhibitors. Bioorg Med Chem. 2015;23:6497-509.

20. Dietrich J, Hulme C, Hurley LH. The design, synthesis, and evaluation of 8 hybrid DFG-out allosteric kinase inhibitors: A structural analysis of the binding interactions of Gleevec ®, Nexavar®, and BIRB-796. Bioorg Med Chem. 2010;18:5738-5748.

21. Domínguez JN, León C, Rodrigues J, De Domínguez NG, Gut J, Rosenthal PJ. Synthesis and evaluation of new antimalarial phenylurenyl chalcone derivatives. J Med Chem. 2005;48:3654-3658.

22. Ismail MMF, Husseiny EM, Ibrahim MH. Mimicry of sorafenib: novel diarylureas as VEGFR2 inhibitors and apoptosis inducers in breast cancer. New Journal of Chemistry. 2023;47:11565-11576.

23. Zhang H, Liu JJ, Sun J, Yang XH, Zhao TT, Lu X, et al. Design, synthesis and biological evaluation of novel chalcone derivatives as antitubulin agents. Bioorg Med Chem. 2012;20:3212-3218.